Original Article

In vivo and *in vitro* investigation of KIN-193 anti-tumor effects on nasopharyngeal carcinoma

Fuhai Chen, Anyuan Zheng, Fen Li, Silu Wen, Shiming Chen, Zezhang Tao

Department of Otolaryngology—Head and Neck Surgery, Renmin Hospital of Wuhan University, Wuhan 430060, China

Contributions: (I) Conception and design: F Chen; (II) Administrative support: S Chen, Z Tao; (III) Provision of study materials or patients: F Chen, A Zheng; (IV) Collection and assembly of data: F Chen, F Li; (V) Data analysis and interpretation: All authors; (VI) Manuscript writing: All authors; (VII) Final approval of manuscript: All authors.

Correspondence to: Zezhang Tao, MD, PhD. Department of Otolaryngology—Head and Neck Surgery, Renmin Hospital of Wuhan University, Wuhan 430060, China. Email: taozezhang@163.com.

Background: The PI3K signaling pathway has important roles in nasopharyngeal carcinoma (NPC) tumorigenesis and progression. Inhibition of the PI3K pathway effectively inhibits NPC growth; however, the toxic side effects of PI3K inhibitors limit their clinical application. This study aimed to investigate the effects of the selective PI3K p110β inhibitor, KIN-193, on proliferation and apoptosis in NPC.

Methods: Cell counting Kit-8, colony formation, flow cytometry, and western blotting experiments were conducted in CNE2Z NPC cells treated with various concentrations of KIN-193 to determine its effects on cell proliferation and apoptosis. Additionally, xenograft tumor models were established in nude mice and the anti-tumor effects of KIN-193 and the classical P110α inhibitor, PIK-75, compared *in vivo*. Hematoxylin-eosin (HE) staining, immunohistochemical staining, and western blotting were also conducted to detect the protein expression levels of proliferation and apoptosis markers.

Results: The results of both *in vivo* and *in vitro* experiments demonstrated that KIN-193 can dramatically inhibit cell proliferation and promote apoptosis in NPC. In addition, KIN-193 showed stronger antitumor effects, with fewer side effects, than PIK-75 *in vivo*.

Conclusions: We conclude that KIN-193 exhibits considerable anti-tumor effects in NPC.

Keywords: p110β inhibitor; nasopharyngeal carcinoma (NPC); proliferation; apoptosis; mice

Submitted Jan 05, 2019. Accepted for publication Oct 30, 2019.

doi: 10.21037/tcr.2019.11.03

View this article at: http://dx.doi.org/10.21037/tcr.2019.11.03

Introduction

Arising from the nasopharyngeal epithelium, nasopharyngeal carcinoma (NPC) is one of the most common head and neck neoplasms, occurring frequently in Southeast Asia, Alaska, and North Africa (1). In China, NPC primarily occurs in the south, including in Guangdong, Guangxi, and Hong Kong (2). Combined radiotherapy and chemotherapy is the standard treatment mode for locally advanced NPC; however, patients suffer poor life quality following treatment, highlighting the need to develop targeted drugs with the aim of improving prognosis (3,4).

The PI3K/Akt/mTOR pathway is involved in a variety of cellular functions, including protein synthesis, cell cycle progression, cell proliferation, apoptosis, and drug resistance. Mammalian Class IA PI3K catalytic subunits include p110α, p110β, p110γ, and p110δ (5). Numerous studies have confirmed that PI3K/Akt/mTOR signaling is activated in multiple tumors (6-9), including in NPC, and inhibition of this pathway can have beneficial therapeutic effects in NPC (10-12). Recent studies have identified various potent inhibitors of PI3K/Akt signaling, which have been widely used in clinical trials (13,14). In particular, the abnormal expression of p110α and p110β, which are encoded by the *PI3CA* and *PI3CB* genes, respectively, has been widely studied and found to regulate the development

of tumors (15), with increased tumor expression of p110β associated with poor prognosis (15,16). While unselective inhibitors of these proteins significantly reduce PI3K/Akt signaling by targeting all p110 subunits, they also cause severe side effects, limiting their clinical application. Molecular therapy targeting the p110β catalytic subunit of PI3K is a promising alternative approach, which may facilitate satisfactory PI3K inhibition with fewer side effects.

KIN-193 is a novel, effective and highly selective p110β inhibitor with an IC50 of 0.69 nM, that has 200, 20, and 70-fold selectivity for p110β over the p110α, p110δ, and p110γ isoforms, respectively. The molecular weight of KIN-193 is 408.45, and its molecular formula is $C_{22}H_{24}N_4O_4$. A literature search indicated that the relationship between KIN-193 and tumors has not been widely investigated or reported. By inhibiting a specific subunit of PI3K, KIN-193 reduces the IC50 of p110β to a minimum and can be applied for the therapy of P110β-dependent tumors, while sparing other PI3K subtypes; thereby reducing the side effects caused by unselective inhibition. Ni *et al.* found that 35% of PTEN mutated cancer cell lines (20 of 57) and 16% of wild-type PTEN cancer cell lines (58 of 365) were sensitive to KIN-193, with an EC_{50} threshold of < 5 μM. Moreover, *in vivo*, all KIN-193-treated mice maintained normal body weights, indicating that KIN-193 was well tolerated in mice and causes fewer side effects (17). This study aimed to investigate the effects of KIN-193 on the proliferation and apoptosis of NPC *in vitro* and *in vivo* to determine whether it is an appropriate potential treatment for NPC.

Methods

Cell culture

The NPC cell line, CNE2Z, was purchased from the Cell Culture Center, Institute of Basic Medicine, Chinese Academy of Medical Sciences (Beijing, China) and cultured in RPMI-1640 medium (Invitrogen Life Technologies, Carlsbad, CA, USA) with 10% fetal bovine serum (Invitrogen Life Technologies, Carlsbad, CA, USA). All cells were cultured at 37 ℃ in 5% CO_2 in a humidified incubator.

Cell proliferation and colony formation assays

Cell proliferation was determined using Cell Counting Kit-8 (Dojindo, Kumamoto, Japan), according to the manufacturer's instructions. For the CCK-8 assay, cells were seeded in 96-well plates at 2.0×10^3 cells per well in RPMI-1640 medium with 10% fetal bovine serum. After a 24 h incubation, cells were treated with KIN-193 (MedChemexpress, Monmouth Junction, NJ, USA) at various concentrations (0, 5, 10, 15, 20, 25, and 30 μM) and incubated in complete medium for 24, 48, or 72 h. Absorbance was measured at 450 nm using a microplate reader (Perkin Elmer, Waltham, MA, USA) at the specified time points (24, 48, or 72 h). For colony formation assays, cells were seeded into 6-well plates (250 cells/well). After incubation for 24 h, cells were treated with various concentrations of KIN-193 (0, 10, 20, and 30 μM) and incubated in complete medium for 12 days. Plates were washed with phosphate buffered saline (PBS; Invitrogen Life Technologies, Carlsbad, CA, USA) and stained with 0.1% Crystal Violet. The number of colonies consisting of >50 cells were calculated. All compounds were dissolved in PBS.

Flow cytometry

Apoptosis was evaluated using the PE Annexin V Apoptosis Detection Kit I (BD Biosciences, San Jose, CA, USA), according to the manufacturer's instructions. Cells were seeded in 6-well plates in RPMI-1640 medium containing 10% fetal bovine serum. After incubation for 24 h, cells were treated with various concentrations of KIN-193 (0, 10, 20, and 30 μM) and incubated in complete medium for 48 h. Then, cells were trypsinized and washed twice with cold PBS. Cells were resuspended in 1 × binding buffer containing 5 μL of annexin V: PE and 5 μL of 7-amino-actinomycin D (7-AAD, used as a nucleic acid dye) (1×10^5 cells/mL) in a total volume of 100 μL, gently mixed, and incubated in the dark for 15 min at room temperature. Binding buffer (1×400 μL) was then added to a clean test tube and the numbers of apoptotic cells quantified by flow cytometry (Becton, Dickinson and Co., Franklin Lakes, NJ, USA) within 1 h. All compounds were dissolved in PBS.

Xenograft study

Four-week-old female BALB/c nude mice were purchased from Beijing Vital River Laboratory Animal Technology Co., Ltd. (Beijing, China) and underwent adaptive feeding a week before the experiment. CNE2Z cells were selected to establish a subcutaneous xenotransplanted tumor model, with 2×10^6 cells suspended in PBS and subcutaneously injected into female BALB/c nude mice in each group. After tumors reached a diameter of ≥0.5 cm, the nude

mice were divided into three groups: (I) receiving PBS (0.2 mL/day); (II) receiving PIK-75 (20 mg/kg/day); and (III) receiving KIN-193 (10 mg/kg/day). Intraperitoneal injections were administered daily and after 8 days of treatment, the mice were sacrificed and tumors surgically removed. During the experiment the longest and shortest dimensions of xenograft tumors were measured once every two days, and tumor volumes calculated using the following equation: volume $=1/2 \times L \times W^2$ (L, length; W, width). Relative tumor volumes were calculated using the following equation: Relative tumor volume (RTV) = V_t/V_0, (V_t, tumor volume measured at each time point; V_0, tumor volume before treatment injection).

Western blotting

CNE2Z cells were treated with KIN-193 at various concentrations and incubated in complete medium for 48 h. CNE2Z cells and tumor tissues were harvested and lysed in buffer supplemented with protease and phosphatase inhibitors (Roche, Basel, Switzerland). Lysates were resolved by SDS-PAGE, then transferred to PVDF membranes (Merck Millipore, Billerica, MA, USA) and immunoblotted with specific primary antibodies. Western blot analysis was performed using the following rabbit antibodies: anti-p110β (1:1,000; Cat. No. 3011), anti-Akt (1:1,000; Cat. No. 4691), anti-phospho-Akt (Thr308) (1:1,000; Cat. No. 13038), anti-Bcl2 (1:1,000; Cat. No. 2872), anti-Bcl-X_L (1:1,000; Cat. No. 2764), anti-Bax (1:1,000; Cat. No. 5023), cleaved anti-Caspase 9 (1:1,000; Cat. No. 20750), anti-GAPDH (1:1,000; Cat. No. 5174), and anti-β-actin (1:1,000; Cat. No. 8457) (polyclonal) (Cell Signaling Technology, Danvers, MA, USA). After immunoblotting with secondary antibodies (donkey anti-rabbit immunoglobulin G; LI-COR, Lincoln, NE, USA), membranes were scanned using an Odyssey infrared imaging system (Biocompare, South San Francisco, CA, USA).

Hematoxylin-eosin (HE) staining

HE staining was conducted according to routine protocols (18).

Immunohistochemical staining

Anti-Akt (1:200; Cat. No. 4691), anti-phospho-Akt (Thr308) (1:2,000; Cat. No. 13038), and anti-Bcl2 (1:2,000; Cat. No. 2872) (polyclonal) (Cell Signaling Technology, Danvers, MA, USA) antibodies were used for immunohistochemical staining, conducted as previously described (19). Staining was analyzed using Image Pro-Plus software (Version 6.0; Media Cybernetics, Silver Springs, MD, USA).

Statistical analysis

All experiments were performed in triplicate. Results are expressed as means ± standard deviations of three independent experiments. P value calculations were conducted using unpaired Student's *t* tests for two group comparisons. All data were analyzed and presented using GraphPad Prism software (version 7.0; La Jolla, CA, USA). $P<0.05$ was considered statistically significant.

Results

KIN-193 inhibited CNE2Z cell proliferation and colony formation and induced their apoptosis

The chemical structure of KIN-193 is shown in *Figure 1A*. CCK-8 and colony formation assays demonstrated that KIN-193 could significantly inhibit CNE2Z cell proliferation and colony formation. Moreover, these effects were enhanced on increasing KIN-193 concentration, indicating a dose-response relationship (*Figure 1B,C*) ($P<0.05$). Western blotting showed reduced p110β expression in cells treated with KIN-193 (*Figure 1D*) ($P<0.05$). Levels of other proliferation markers, including phospho-Akt, also decreased in response to increasing concentrations of KIN-193 (*Figure 1D*) ($P<0.05$); however, overall levels of Akt did not alter in response to KIN-193 administration (*Figure 1D*). CNE2Z cells underwent dramatic apoptosis in response to increasing concentrations of KIN-193, as demonstrated by flow cytometry (*Figure 1E*) ($P<0.05$). Protein markers of apoptosis, such as Bax and cleaved Caspase 9, were expressed at higher levels in the KIN-193-treated group than in controls; however, levels of Bcl-X_L showed the opposite response, with markedly and significantly reduced levels (*Figure 1F,G*) ($P<0.05$).

Protein expression differences among mice with xenografted tumors, comparison of tumor volumes and HE staining

Tumor xenografts from mice treated with KIN-193 expressed less p110β (*Figure 2A*), as well as p-Akt (*Figure 2A*), Bcl-2, and Bcl-X_L (*Figure 2B*), compared with

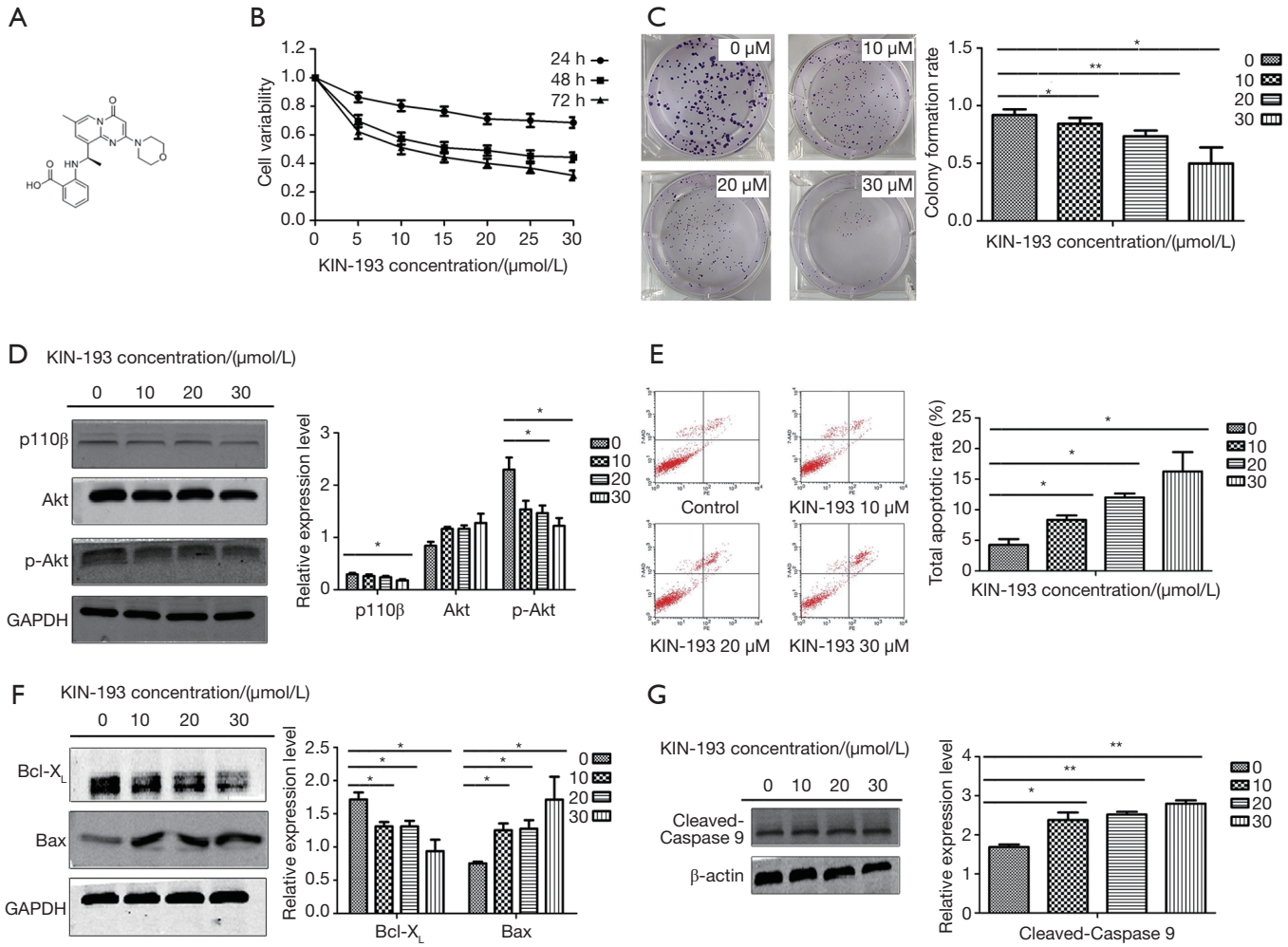

Figure 1 KIN-193 inhibits the proliferation of CNE2Z cells and induces their apoptosis. (A) The chemical structure of KIN-193; (B) cells were treated with different concentrations of KIN-193 for 24, 48, and 72 h, and then cell viability was assayed using the CCK-8 Kit; (C) colony formation assays were performed to examine the colony formation ability of CNE2Z cells (Annexin PE/7-AAD staining) treated with different concentrations of KIN-193; (D) effect of KIN-193 on expression of proteins related to cell proliferation in CNE2Z cells. Western blotting showed that drug-treated CNE2Z cells exhibited significant differences in p110β and p-Akt expression levels, compared with the control group; (E) effect of KIN-193 on CNE2Z cell apoptosis. Apoptotic status was determined by Annexin PE/7-AAD staining. Drug-treated CNE2Z cells showed significantly increased apoptosis; (F,G) effect of KIN-193 on expression of proteins related to apoptosis in the CNE2Z cells. Western blotting showed that drug-treated CNE2Z cells had significant differences in Bcl-X_L, Bax, and cleaved-Caspase 9 expression levels compared with the control group. *, P<0.05 *vs.* the control group; **, P<0.01 *vs.* the control group.

those from control mice (P<0.05). Apoptosis markers, including Bax and cleaved Caspase 9, were significantly upregulated in both the PIK-75 and KIN-193 groups (*Figure 2B,C*) (P<0.05). No differences in Akt expression were observed among the three groups (*Figure 2A*). Relative tumor volume was significantly lower in the KIN-193 group compared with the PBS group (*Figure 2D*) (P<0.05). Moreover, relative to the control group, keratin pearls appeared more frequently in the PIK-75 group, and at even higher levels in the KIN-193 group (*Figure 2E*).

IHC staining of tumor xenografts

Compared with the PBS control group, the PIK-75 and KIN-193 groups expressed significantly lower levels of phospho-Akt (*Figure 3A,B*) and Bcl2 (*Figure 3A,C*); however,

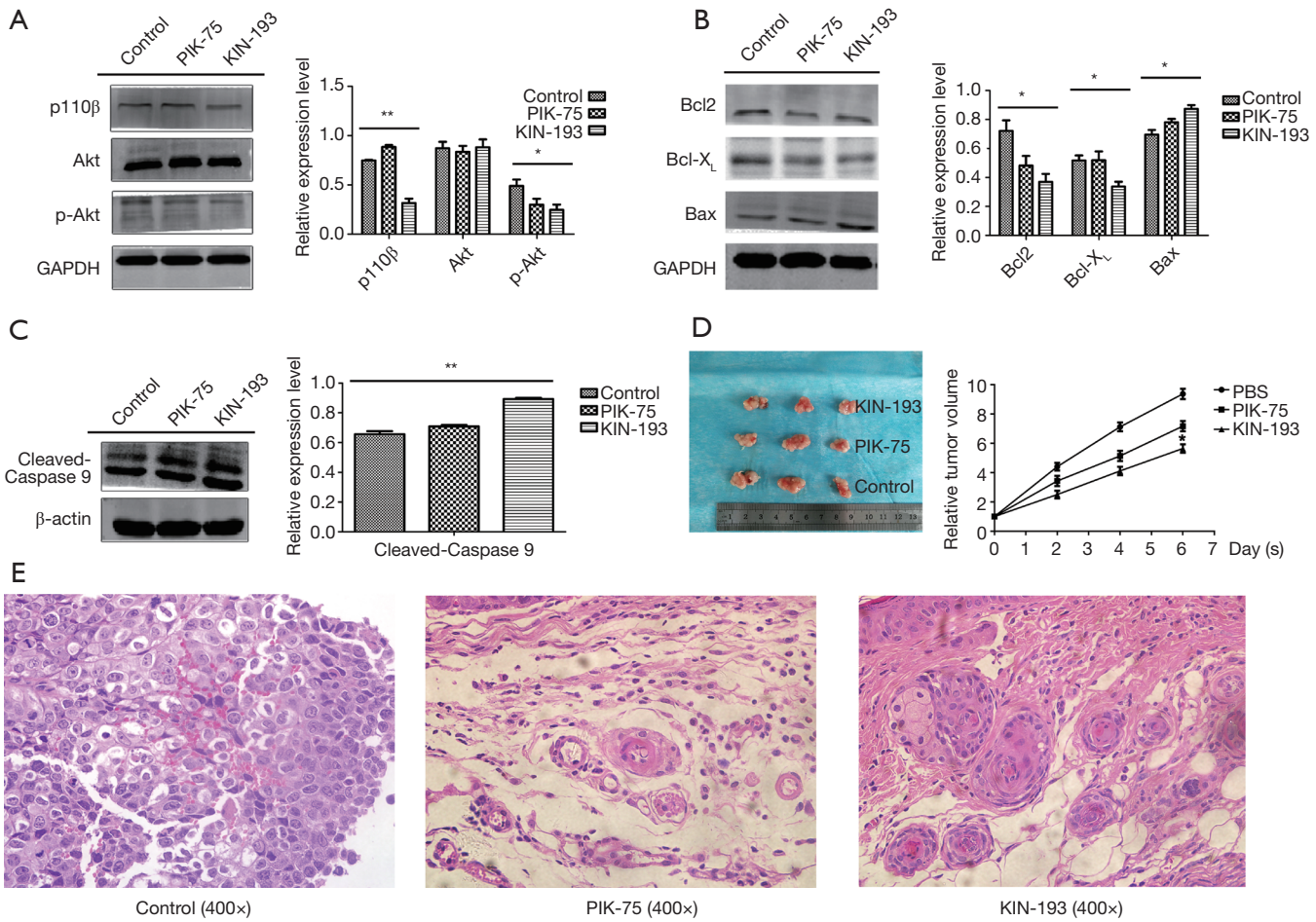

Figure 2 Protein expression differences among mice with tumor xenografts, comparison of tumor volume and HE staining. (A) Western blotting was performed to examine the levels of proteins related to cell proliferation (p110β, Akt, and p-Akt) in tumor xenografts from mice treated with PBS, PIK-75, and KIN-193; (B,C) western blotting was performed to examine the levels of proteins associated with apoptosis (Bcl2, Bcl-X_L, Bax, and cleaved-Caspase 9) in tumor xenografts from mice treated with PBS, PIK-75, and KIN-193; (D) tumor volumes were calculated (left) and a line chart constructed (right). Experimental groups were as follows: PBS (control, bottom), PIK-75 (p110α inhibitor, middle), and KIN-193 (p110β inhibitor, upper); (E) HE staining of xenografted tumors. Experimental groups were as follows: PBS (control, left), PIK-75 (p110α inhibitor, middle), and KIN-193 (p110β inhibitor, right). *, P<0.05 *vs.* the control group; **, P<0.01 *vs.* the control group. HE, hematoxylin-eosin.

Akt expression was not affected among the three groups (*Figure 3A,D*) (P<0.05).

Discussion

The reagent used in this investigation, KIN-193, is a highly selective p110β inhibitor, which can reduce tumor cell proliferation by blocking the PI3K/Akt signaling pathway. Previous studies have shown that inhibition of PI3K/Akt signaling can effectively inhibit the proliferation of NPC (10-12). Using Cell Counting Kit-8 and colony formation assays, we observed a decrease in the proliferation capacity of CNE2Z cells in response to increasing concentrations of KIN-193, which is consistent with the results of previous studies. Overexpression of Akt does not transform normal cells to produce a malignant phenotype; however, overexpression of phospho-Akt can cause phosphorylation of more than 20 downstream substrate molecules, thereby promoting cell growth, proliferation, invasion, and migration (20). To explore the effects of KIN-193 on

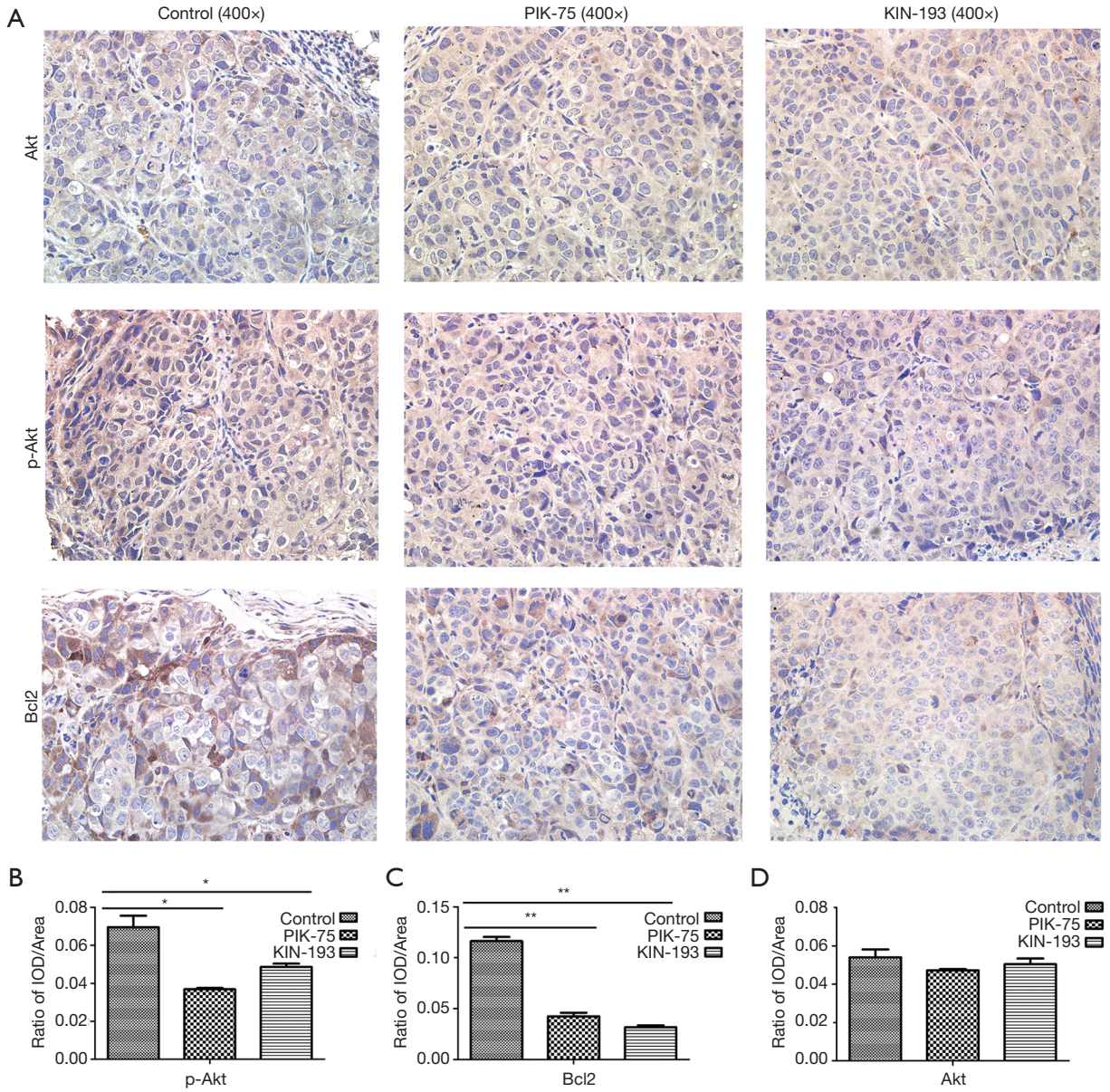

Figure 3 Expression levels of Akt, p-Akt, and Bcl2 in mice with tumor xenografts determined by IHC staining. (A) Expression levels of proteins detected by IHC. Experimental groups were as follows: PBS (left), PIK-75 (middle), and KIN-193 (right). IHC detected the expression of Akt (upper), p-Akt (middle), Bcl2 (lower); (B,C,D) IHC images were analyzed using Image Pro-Plus 6.0 and bar graphs generated (Integrated option density, IOD). *, P<0.05 *vs.* the control group; **, P<0.01 *vs.* the control group.

p110β, Akt, and phosphorylated Akt in NPC, we performed western blotting using CNE2Z cells and transplanted tumor tissues and found that KIN-193 could significantly down-regulate p110β and phospho-Akt, both *in vivo* and *in vitro*. Moreover, this down-regulation was enhanced by increasing KIN-193 concentration. These data suggest that the PI3K/Akt pathway contributes to NPC tumorigenesis, and that KIN-193 can reverse its effects. In contrast, overall Akt expression was not affected by KIN-193; therefore, we speculate that unphosphorylated Akt may not contribute to the anti-proliferation mechanism of KIN-193 treatment, and that KIN-193 anti-proliferative activity may be related to activation of the PI3K/Akt signaling pathway.

Tumorigenesis is not only caused by abnormal cell

proliferation, but also by dysregulation of apoptosis, since inhibition of apoptosis that cannot be recovered causes cells to proliferate uncontrollably, promoting tumor formation. In this study, we found that KIN-193 also significantly induced NPC cell apoptosis. Apoptosis regulators of the Bcl family, among which Bcl2, Bcl-X_L, and Bax are major representatives, can be divided into apoptosis suppressors and apoptosis promoters (21). Bcl2 is a 27 kDa intracellular membrane protein, which localizes to mitochondria and smooth endoplasmic reticulum, along with reactive oxygen species (ROS), and inhibits the apoptosis induced by these oxidizing agents. Previous investigations have demonstrated that Bcl2 can prolong cell survival and inhibit apoptosis; the subcellular distribution and functions of Bcl-X_L are similar to those of Bcl2 (22). Bax is an important dimer that promotes apoptosis. Pepper *et al.* found that overexpression of Bcl2 can induce its formation of heterodimers with Bax, to inhibit apoptosis; hence, the ratio of Bcl2 and Bax is an important index that assists in judging drug resistance and predicting malignant tumor recurrence (23). Further, Sedlak *et al.* discovered that Bcl-X_L can form heterodimers with Bax in mammalian cells and that their ability to combine can be abrogated by substitution of a single amino acid, leading to cell proliferation (24). Furthermore, in NPC, Bcl2 is usually expressed at high levels (25,26), with Bax expressed at low levels (27); therefore, we explored the expression levels of Bcl2, Bcl-X_L, and Bax in CNE2Z cells and tumor xenografts to evaluate the curative effects of KIN-193. Our western blotting experiments demonstrated that expression levels of Bcl2 and Bcl-X_L were down-regulated, while those of Bax were up-regulated in CNE2Z cells and CNE2Z-transplanted tumor tissue in response to KIN-193 treatment, which would be expected to result in increased levels of heterologous Bcl2 dimers and a decrease in levels of homodimers; thereby, promoting apoptosis. We also detected Bcl2 expression in xenografted tumor cells using IHC to evaluate the influence of KIN-193 on Bcl2 *in vivo*. Our data clearly show that KIN-193 can dramatically reduce numbers of Bcl2-positive cells in tumors and ultimately induce tumor cell death. These results are consistent with those reported by Pepper *et al.* and Sedlak *et al.* (23,24). Hilchie *et al.* proposed that oligomerization of the pro-apoptotic molecule, Bax, occurs after cells receive apoptotic signals; the oligomers then transfer to the mitochondrial outer membrane, where they bind to voltage-dependent anion channels, leading to the release of cytochrome C and apoptosis (28). Based on the above experimental results and reported theoretical analysis, we conclude that KIN-193 may mediate mitochondrial outer membrane permeability by down-regulating Bcl-2 and up-regulating Bax protein expression.

As mentioned above, Bax alters mitochondrial permeability after receiving an apoptotic signal, opening the mitochondrial channel, leading to the release of pro-apoptotic substances and activation of the caspase family. Extracellular signals activate the apoptotic enzyme, caspase, within cells, leading to apoptosis and DNA damage. Caspase 9 is a member of the caspase family and an initiator of apoptosis, which can stimulate the apoptotic pathway, thereby activating Caspase 3, further inducing enzyme inactivation related to gene repair and the cell cycle, and ultimately leading to apoptosis. Western blotting of samples from *in vivo* and *in vitro* experiments revealed that treatment with KIN-193 led to dose-responsive cleavage of Caspase 9 into its active subunit, accelerating apoptosis. Therefore, KIN-193 may regulate CNE2Z apoptosis by activating the caspase cascade. Our results indicate that the pro-apoptosis function of KIN-193 is related to activation of Bcl2, Bax, and Caspase 9.

One characteristic of tumor cells is that they undergo dedifferentiation, where they effectively transform into stem cells. In general, poorly differentiated tumors are more malignant. Pathological studies have shown that lamellar keratin can be detected in the center of well-differentiated squamous cell carcinomas, which is referred to as the formation of keratin pearls. CNE2Z is a poorly differentiated NPC cell line, derived from a head and neck squamous cell carcinoma. Compared with the control group, keratin pearls were more common in the PIK-75 and KIN-193 groups in HE stained samples, and there were relatively more keratin pearls in the KIN-193 group. This indicates that the tumors from nude mice treated with KIN-193 change from being poorly differentiated to become highly differentiated, and suggests that KIN-193 may reduce the malignant potential of CNE2Z cells by changing their degree of differentiation.

Conclusions

As a selective PI3K/Akt pathway inhibitor, KIN-193 can clearly inhibit the proliferation of NPC cells and induce their apoptosis. Our research offers not only a theoretical foundation for the clinical application of a new PI3K inhibitor but also has potential to increase the breadth of choice of personal therapeutic schedules for patients with NPC.

Acknowledgments

This work was supported by the National Natural Science Foundation of China (No. 81372880; No. 81670910) and the Guidance fund of the Renmin Hospital of Wuhan University (No. RMYD2018Z12).
Funding: None.

Footnote

Conflicts of Interest: All authors have completed the ICMJE uniform disclosure form (available at http://dx.doi.org/10.21037/tcr.2019.11.03). The authors have no conflicts of interest to declare. Institutional ethical approval and informed consent were waived.

Ethical Statement: The authors are accountable for all aspects of the work in ensuring that questions related to the accuracy or integrity of any part of the work are appropriately investigated and resolved. The study was conducted in accordance with the Declaration of Helsinki (as revised in 2013). The institutional ethical approval was waived. The animal experiment was conducted in compliance with the national and institutional guidelines for the care and use of animals.

References

1. Siegel RL, Miller KD, Jemal A. Cancer statistics, 2018. CA Cancer J Clin 2018;68:7-30.
2. Wei KR, Zheng RS, Zhang SW, et al. Nasopharyngeal carcinoma incidence and mortality in China in 2010. Chin J Cancer 2014;33:381-7.
3. Qiu WZ, Ke LR, Xia WX, et al. A retrospective study of 606 cases of nasopharyngeal carcinoma with or without oropharyngeal candidiasis during radiotherapy. PLoS One 2017;12:e0182963.
4. Siegel RL, Miller KD, Jemal A. Cancer Statistics, 2017. CA Cancer J Clin 2017;67:7-30.
5. Vanhaesebroeck B, Guillermet-Guibert J, Graupera M, et al. The emerging mechanisms of isoform-specific PI3K signalling. Nat Rev Mol Cell Biol 2010;11:329-41.
6. Chen D, Lin X, Zhang C, et al. Dual PI3K/mTOR inhibitor BEZ235 as a promising therapeutic strategy against paclitaxel-resistant gastric cancer via targeting PI3K/Akt/mTOR pathway. Cell Death Dis 2018;9:123.
7. Hua H, Zhu Y, Song YH. Ruscogenin suppressed the hepatocellular carcinoma metastasis via PI3K/Akt/mTOR signaling pathway. Biomed Pharmacother 2018;101:115-22.
8. Liu F, Gao S, Yang Y, et al. Antitumor activity of curcumin by modulation of apoptosis and autophagy in human lung cancer A549 cells through inhibiting PI3K/Akt/mTOR pathway. Oncol Rep 2018;39:1523-31.
9. Yanwei L, Yinli Y, Pan Z. Traditional Herbal Formula NPC01 Exerts Antiangiogenic Effects through Inhibiting the PI3K/Akt/mTOR Signaling Pathway in Nasopharyngeal Carcinoma Cells. Evid Based Complement Alternat Med 2018;2018:5291517.
10. Li SS, Yang S, Yin DH, et al. [Inhibition of PI3K-Akt pathway reverses LMP1 induced TRAIL resistance in nasopharyngeal carcinoma cell]. Lin Chung Er Bi Yan Hou Tou Jing Wai Ke Za Zhi 2016;30:744-7.
11. Wong CH, Ma BB, Cheong HT, et al. Preclinical evaluation of PI3K inhibitor BYL719 as a single agent and its synergism in combination with cisplatin or MEK inhibitor in nasopharyngeal carcinoma (NPC). Am J Cancer Res 2015;5:1496-506.
12. Liu T, Sun Q, Li Q, et al. Dual PI3K/mTOR inhibitors, GSK2126458 and PKI-587, suppress tumor progression and increase radiosensitivity in nasopharyngeal carcinoma. Mol Cancer Ther 2015;14:429-39.
13. Massacesi C, Di Tomaso E, Urban P, et al. PI3K inhibitors as new cancer therapeutics: implications for clinical trial design. Onco Targets Ther 2016;9:203-10.
14. Greenwell IB, Flowers CR, Blum KA, et al. Clinical use of PI3K inhibitors in B-cell lymphoid malignancies: today and tomorrow. Expert Rev Anticancer Ther 2017;17:271-9.
15. Wu S, Li T, Mu Q, et al. Expression of PI3Kp110alpha and PI3Kp110beta in the colorectal conventional adenoma, serrated lesions and adenoma with canceration and their significance. Int J Clin Exp Pathol 2015;8:16026-35.
16. Li SM, Wu SH. [Expression and clinical significance of epidermal growth factor receptorHER2, PI3Kp110alpha and PI3Kp110beta in gastric carcinoma]. Zhonghua Bing Li Xue Za Zhi 2016;45:407-8.
17. Ni J, Liu Q, Xie S, et al. Functional characterization of an

isoform-selective inhibitor of PI3K-p110beta as a potential anticancer agent. Cancer Discov 2012;2:425-33.
18. Guo Y, Wang L, Ma R, et al. JiangTang XiaoKe granule attenuates cathepsin K expression and improves IGF-1 expression in the bone of high fat diet induced KK-Ay diabetic mice. Life Sci 2016;148:24-30.
19. Otali D, Fredenburgh J, Oelschlager DK, et al. A standard tissue as a control for histochemical and immunohistochemical staining. Biotech Histochem 2016;91:309-26.
20. Martini M, De Santis MC, Braccini L, et al. PI3K/AKT signaling pathway and cancer: an updated review. Ann Med 2014;46:372-83.
21. Korsmeyer SJ. Bcl-2 initiates a new category of oncogenes: regulators of cell death. Blood 1992;80:879-86.
22. González-García M, Perez-Ballestero R, Ding L, et al. bcl-XL is the major bcl-x mRNA form expressed during murine development and its product localizes to mitochondria. Development 1994;120:3033-42.
23. Pepper C, Bentley P, Hoy T. Regulation of clinical chemoresistance by bcl-2 and bax oncoproteins in B-cell chronic lymphocytic leukaemia. Br J Haematol 1996;95:513-7.
24. Sedlak TW, Oltvai ZN, Yang E, et al. Multiple Bcl-2 family members demonstrate selective dimerizations with Bax. Proc Natl Acad Sci U S A 1995;92:7834-8.
25. Li Y, Yan L, Zhang W, et al. miR-21 inhibitor suppresses proliferation and migration of nasopharyngeal carcinoma cells through down-regulation of BCL2 expression. Int J Clin Exp Pathol 2014;7:3478-87.
26. Kontos CK, Fendri A, Khabir A, et al. Quantitative expression analysis and prognostic significance of the BCL2-associated X gene in nasopharyngeal carcinoma: a retrospective cohort study. BMC Cancer 2013;13:293.
27. Zhou Z, Meng M, Ni H. Chemosensitizing Effect of Astragalus Polysaccharides on Nasopharyngeal Carcinoma Cells by Inducing Apoptosis and Modulating Expression of Bax/Bcl-2 Ratio and Caspases. Med Sci Monit 2017;23:462-9.
28. Hilchie AL, Furlong SJ, Sutton K, et al. Curcumin-induced apoptosis in PC3 prostate carcinoma cells is caspase-independent and involves cellular ceramide accumulation and damage to mitochondria. Nutr Cancer 2010;62:379-89.

Cite this article as: Chen F, Zheng A, Li F, Wen S, Chen S, Tao Z. *In vivo* and *in vitro* investigation of KIN-193 anti-tumor effects on nasopharyngeal carcinoma. Transl Cancer Res 2020;9(1):49-57. doi: 10.21037/tcr.2019.11.03

